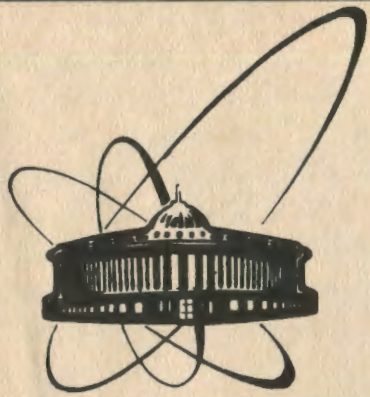

сообщения
объединенного
института
ядерных
исследований
дубна

E6-90-477

A.Kovalik, V.M.Gorozhankin, A.F.Novgorodov,
M.A.Mahmoud, A.Minkova, G.J.Beyer, H.Ravn,
Li Yong Il

THE K AUGER SPECTRUM OF KRYPTON FROM THE ^{83}Rb DECAY

1990

INTRODUCTION

In the past, both experimental and theoretical investigations of the K Auger transitions in the elements were concentrated mainly on the most intensive and relatively simple KLL spectrum. Nevertheless, even this activity has not brought the theory into complete agreement with experiment (see e.g. [1]). New experimental data of a very high quality are desirable in the Z = 10 - 40 region and for the heaviest elements as well as on the weak satellite line intensities. The other K Auger spectra were measured rarely (e.g. [2,3]) due to their complexity and small intensity. Theoretical material devoted to the KLX (KLX=KLM+KLN) and KMX (KMX=KMM+KMN) spectra is scarce, too.

Experimental information on K Auger transitions in noble gases is of special importance for a comparison with theoretical predictions. Approximations assumed in the calculations of Auger transition energies and intensities are the most justified in these atoms (e.g. closed atomic orbitals, negligible chemical effects).

In the present paper, we report preliminary results on the experimental study of the K Auger electrons emitted during the electron capture decay of $^{83}_{37}Rb$ ($T_{1/2}$=86.2 d) into $^{83}_{36}Kr$. To our knowledge, the spectrum is studied for the first time.

EXPERIMENTAL

Source preparation

The ^{83}Rb isotope was induced by irradiation of a massive niobium target on the installation ISOLDE-2 (CERN, Switzerland) using 600 MeV protons. The ions of A=83 were implanted into an aluminium foil of 100 μm thickness. The

mass separated sample contained less than 0.008% of ^{84}Rb.

The aluminium foil was firstly diluted in 1 M hydrochloric acid. After the precipitation of aluminium hydroxide by means of ammonia, the centrifugate was volatilized to dryness and the ammonium chloride was removed by the subsequent heating. The chemical concentration was carried out in quartz vessels using double-distilled water and reagents of a special purity. The final purification of rubidium from light alkali elements was done on a microchromatography column (2x40 mm) filled with cationic exchanger OSTION LG KS 0803. The eluation was performed by the nitric acid solutions of increasing concentrations (from 0.3 M up to 2.0 M). Practically, the whole ^{83}Rb isotope was washed-out in 2-3 drops that were subsequently volatilized on an annealed Ta boat.

Radioactive sources of ^{83}Rb (three in all) for electron spectrum measurements were prepared by an evaporation in vacuum of 10^{-5} torr. To release some impurities, the boat with the activity was heated to 100-200 ^{o}C for 10 minutes. During the treatment, the Al mirror-like hemispherical source backing (formerly cleaned in spirit by ultrasonics) was situated outside the boat. The source evaporation took about one minute at 800 ^{o}C. The deposites of 8 mm diameter were invisible. The most intensive source ($\sim$ 350 μCi) of a suitable quality was chosen for the measurements.

Spectrum measurements

The electron spectra were analysed using the electrostatic spectrometer [4] at the JINR in Dubna modified in october 1989. The analyser slits of about 20 mm widths were covered by Ta wires of 0.1 mm diameter with the step of 1.5 mm to minimize the electrostatic field deformation. Owing to this, the instrumental resolution increased by a factor of 2 or, at the same retardation ratio, the luminosity of the whole spectrometer set up increased by a factor of 3. No

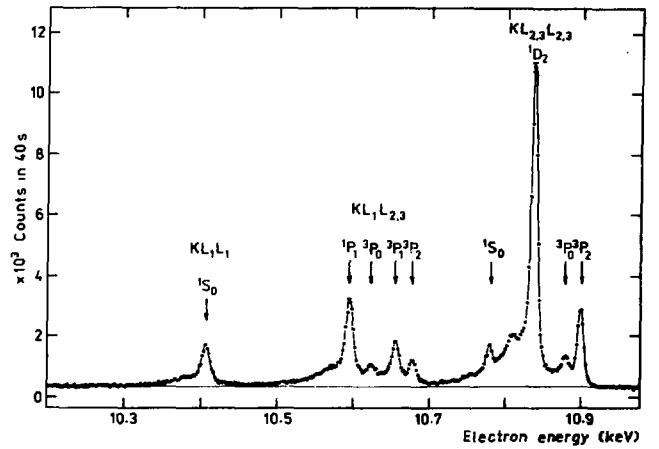

Fig.1. Example of the KLL Auger spectrum of krypton (Z=36) taken at the instrumental resolution of 6.5 eV and the step of 2 eV.

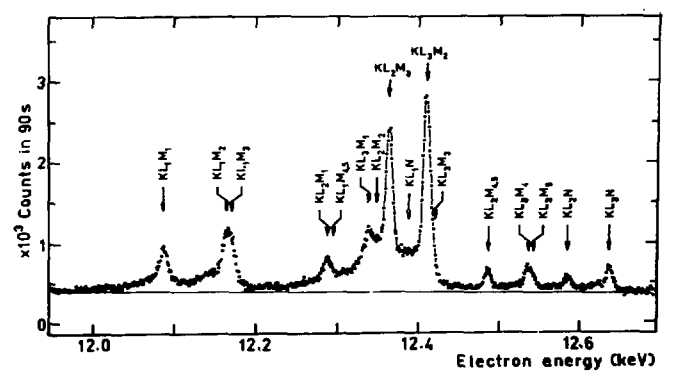

Fig.2. The KLX Auger spectrum of krypton recorded at the 6.5 eV instrumental resolution and the step of 1 eV.

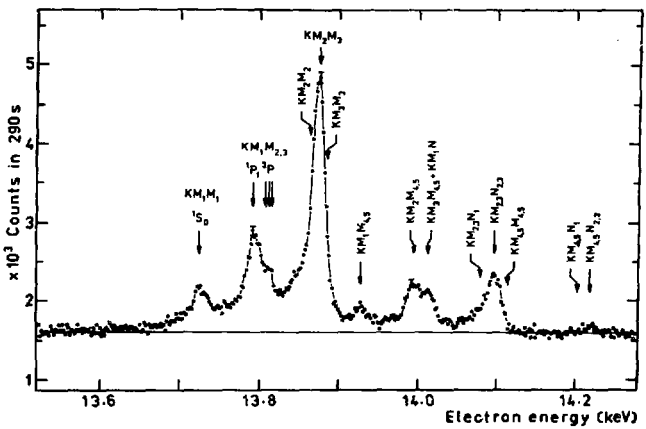

Fig.3. The KMX Auger spectrum of krypton measured at the instrumental resolution of 12 eV and the step of 2 eV. The spectrum is the sum of three independent measurements.

other significant changes of the spectrometer parameters were found.

The majority of the measurements were carried out at the instrumental resolution of 6.5 eV (i.e. at the electron deceleration down to about 200 eV) and the energy step of 2 eV. The KMX spectrum was also taken at the lower electron retardation (to 400 and 500 eV) to compensate for its very low intensity and to improve the peak-to-background ratio. This ratio was unfavourable throughout the all measurements due to the high intrinsic noise of the channeltron caused probably by the age degradation of its performance. (The application of the treatment [5] by both the cold caustic soda and isopropyl alcohol under ultrasonics did not restore original properties of the detector.) Because of high channeltron background, we were not able to take the KMX spectrum of very high quality. In addition, one KLL spectrum was measured at the 4 eV instrumental resolution. Some narrow

sections of the K Auger spectrum were taken, moreover, at better resolutions and finer steps to obtain more accurate information on relative intensities and energy separations of the weak spectrum components. The exposure time per point ranged from several second for the KLL spectrum to about 200 seconds for the KMX one. Examples of the measured spectra are shown in Figs. 1-3.

Energy calibration

The energy calibration of the spectrometer was accomplished employing the following conversion electron lines:

i) K, L_1 and M_1 of the 14.41302(32) keV [6] nuclear transition in ^{57}Fe,

ii) M_1 and L_1, L_2, M_1, M_2 of the 8.41008(21) keV [7] and 20.74378(10) keV [8] transitions, respectively, in ^{169}Tm,

iii) K and M_3 of the 60.0100(18) keV [9] and 18.764(2) keV [10] transitions, respectively, in ^{155}Gd.

In the measurements, the ^{83}Rb source was alternated with the "calibration" ones (^{57}Co, ^{169}Yb or ^{155}Eu) prepared also by the vacuum evaporation on the Al backings. To eliminate possible influences of the source exchanges and likely various chemical environments of the examined radioactive isotopes, we carried out a series of measurements with a combined ^{83}Rb + ^{57}Co + ^{169}Yb evaporated source on the Al backing, too. The line positions remained unaffected within the experimental uncertainties. We have found that the calibrations by means of ^{57}Co and ^{155}Gd isotopes are consistent with each other, while the calibration by ^{169}Tm decreased electron line energies by the value of about 2 eV. The cause of the discrepancy is not evident.

SPECTRUM ANALYSIS

To decompose the spectra into components, the computer

code [11] was used applying the same procedure as in our previous works (e.g. [12]). We treated six KLL, eight KLX and five KMX spectra. It was found that the high energy side, particularly of the KLL lines taken at the instrumental resolution of 6.5 eV or better, can hardly be approximated by a Gauss function (used in our data processing as the main component of the fitted single line shape). This indicated that the values of the absolute instrumental resolution and the natural energy widths of the lines were close to each other. In order to derive information on K Auger line widths, we employed the procedure and the computer code [13]. In this method, the high energy side of the measured line is described by a convolution of the Gaussian and the Lorentzian functions. The former curve approximates the spectrometer response to monoenergetic electrons while the latter one represents the electron energy distribution of the particular Auger line. The values of both the instrumental resolution and the natural line width were varied during the fitting. The weighted averages of the energies and relative intensities of the krypton K Auger lines as well as some of their natural energy widths are summarized in Tables 1-5. The uncertainties given are our estimates of standard deviations (σ).

RESULTS AND DISCUSSION

Energies

The absolute energies of the most intense components of the individual K Auger groups referenced to the Fermi level are presented in Table 1. In the estimation of the quoted errors, we also considered the above mentioned discrepancy in the calibration as well as the possible chemical shifts [14] of the electron binding energies [15]. (The shifts were not taken into account in the determination of the calibration conversion line positions since the chemical states of the

Table 1
Absolute and relative energies of the dominant K Auger transitions in krypton (eV)

Transition	Absolute energy			Relative energy	
	Experiment This work	Theory Ref.16	Exp-Th	Experiment This work	Theory Ref.16
$KL_2L_3(^1D_2)$	10837.4(10)[a]	10824.9	+12.5	0.0	0.0
$KL_3M_2(^3P_2)$	12409.1(15)	12396.8	+12.3	+1572.0(4)	+1571.9
$KM_2M_3(^1D_2)$	13876.0(15)	13862.6	+13.4	+3037.8(8)	+3037.7

[a] 10837.4(10) means 10837.4 ± 1.0.

isotopes in the sources were not exactly known.) The semiempirical predictions of Larkins [16] (also presented in the table) were calculated for the vapor-phase system and are therefore referenced to the vacuum level.

As can be seen, the experimental and theoretical energy differences from the $KL_2L_3(^1D_2)$ line are in a very good agreement whereas the predicted absolute energies are lowered by almost the same value for all lines. According to the theory [16], an adoption of the vapor-phase data for the solid phase system increases the absolute energies equally for all Auger transitions. Thus the solid states effects in the ^{83}Rb source apparently induced the observed disagreement. Likely, doughter ^{83}Kr atoms remain in bounded states after the ^{83}Rb decay. The conversion electron measurements [17] support this conclusion.

The experimental relative energies of the KLL transitions (except the $KL_3L_3(^3P_0)$ one) systematically exceed the calculated ones [16] (Table 3a) by 4-6 σ. The similar discrepancies were found also for another nearby elements (e.g. arsenic [18], bromine [19]). The relative energy of -369 ± 5 eV measured for the $KL_1L_1(^1S_0)$ transition in Br [19] is lower by 36 eV than the estimation [16] and

seems to be erroneous. From the measurements at the higher resolution, we determined the energy splitting of the krypton KL_1L_2 and KL_1L_3 doublets to be 27.7(7) eV and 21.9(6) eV, respectively. The corresponding semiempirical values are 31.5 eV and 22.5 eV [16], respectively.

The energy spacings of the KLM and KMX lines (Tables 4a, 5a) obtained from the measurements and the calculations [16] are in a very good accord with each other for almost all resolved components. The value of 6.9 eV predicted by [16] for the $KL_1M_2(^1P_1)$-$KL_1M_3(^3P_1)$ line separation agrees with the experimental one of 7.5 ± 1.0 eV. The observed splitting of the $KL_3M_{4,5}$ line (see also Fig.2) demonstrates the influence of the intermediate coupling effects on the structure of the KLM spectrum.

Natural widths

In the limit of the jj coupling, the natural width of a K Auger line should be the sum of the natural widths of the participating atomic shells and/or subshells. Values obtained in this way for krypton are presented in Table 2 as "estimated " together with the measured and semiempirical [20] ones. In the estimation, we used experimental values of 2.5(2), 4.5(3), 1.0(4), 1.2(2) and 3(1) eV for the krypton K, L_1, L_2, L_3 and M_3 atomic level widths, respectively,

Table 2
Natural widths of some krypton K Auger lines (eV)

Line	KL_1L_1	KL_1L_3	KL_2L_3	KL_3L_3	$KL_3M_{2,3}$
Measured	9(1)	8.6(8)	4.3(7)	5.2(3)	7.0(9)
Estimated[a]	11.5(5)	8.2(4)	4.7(5)	4.9(4)	6.7(10)
Calculated[b]	11.3(23)	8.3(13)	5.2(5)		

[a] The linear addition of the experimental atomic level widths [17](see text).

[b] Ref.20.

determined in [17] by means of the conversion electron lines of the 9.4 keV nuclear transition in ^{83m}Kr. The measured Auger line widths (the weighted means of five to nine independent values) are in a good agreement with the other ones except the KL_1L_1 component.

Intensities

KLL spectrum

The measured KLL transition rates in reference to the total KLL strength are compared in Table 3a with both the relativistic calculations in intermediate coupling with configuration mixing by Chen et al. [1] and the values [21] obtained by a polynomial fit to the experimental data. As can be seen, the predicted intensities [1] for the $KL_1L_1(^1S_0)$ and $KL_1L_2(^1P_1)$ transitions are higher by 3σ and 7σ, respectively, while that for the $KL_2L_3(^1D_2)$ line is lower by more than 2σ. The deviation of the theory [1] from experiment for krypton is similar to that observed for another light elements (e.g. Fe [12], Mn [22], As [18], Br [19]). The theory of Chen et al. failed also in the prediction of the $KL_1L_2(^3P_0)/(^1P_1)$ satellite-to-main-line intensity ratio; the measured value of 0.146(11) (obtained from special measurements) exceeds by 4σ the theoretical one of 0.104. For the other doublets, the estimated values of 0.529 and 0.243 for the $KL_1L_3(^3P_2)/(^3P_1)$ and $KL_3L_3(^3P_0)/(^3P_2)$ intensity ratios, respectively, reach within 2σ the measured ones of 0.526(21) and 0.232(23), respectively. From Table 3b, it is seen, moreover, that the calculations [1] overestimate the transition intensities to the $(2s)^0(2p)^6$ and $(2s)^1(2p)^5$ configurations and underestimate that to the $(2s)^2(2p)^4$ one. The same trend was found for As [18] and Br[19]. The predictions of the non-relativistic calculations in intermediate coupling with configuration interaction [23] are closer to the measurement. On the other hand, the data [21] derived from experiment agree within 2σ with our results except the $KL_3L_3(^3P_2)$

Table 3a

Relative energies and intensities of the KLL Auger transitions in krypton

Transition	Energies (eV)		Intensities (%)[a]		
	Experiment	Theory	Experiment	Theory	
	This work	Ref.16	This work	Ref.1	Ref.21[b]
$KL_1L_1(^1S_0)$	-430.5(6)	-426.7	6.8(3)	7.71	6.9(6)
$KL_1L_2(^1P_1)$	-241.8(4)	-240.0	13.9(3)	16.08	14.3(15)
$KL_1L_2(^3P_0)$	-213.5(9)	-208.5	2.1(2)	1.67	1.9(9)
$KL_1L_3(^3P_1)$	-181.8(5)	-178.7	6.4(2)	6.34	6.0(21)
$KL_1L_3(^3P_2)$	-159.9(8)	-156.2	3.5(2)	3.35	3.3(14)
$KL_2L_2(^1S_0)$	-58.8(6)	-55.4	3.5(2)	3.54	3.9(4)
$KL_2L_3(^1D_2)$	0.0	0.0	48.9(8)	47.01	50.4(24)
$KL_3L_3(^3P_0)$	+42.5(5)	+42.6	2.7(2)	2.79	2.8(9)
$KL_3L_3(^3P_2)$	+62.4(4)	+60.4	12.2(3)	11.49	10.5(17)

[a] Normalized to ΣKLL.

[b] The fit to the experimental data.

Table 3b

Krypton relative transition intensities associated with the individual electron configurations

Configuration	Experiment	Theory		
	This work	Ref.23[a]	Ref.1	Ref.21[b]
$(2s)^0(2p)^6$	6.8(3)	5.84	7.77	6.9(6)
$(2s)^1(2p)^5$	25.9(5)	25.40	27.51	25.5(31)
$(2s)^2(2p)^4$	67.3(9)	68.77	64.72	67.6(31)

[a] Z=35. [b] The fit to the experimental data.

transition. (Intensities of this component were extracted in [21] from those for the KL_3L_3 doublets experimentally hardly resolved in the low Z region.) The disagreement found between our measurement and the theory [1] for the KLL spectrum of krypton indicates again (e.g. [12,22]) that the approach [1] needs an improvement.

KLX spectrum

The KLX spectrum was decomposed into ten and sixteen components the relative intensities of which are presented in Table 4a. The only transition probability calculations performed for the complete KLX spectrum are the relativistic ones in the jj coupling of Chen et al. [25]. Their predictions for krypton are also given in the table. It is seen that the theory [25] differ significantly from experiment especially for the KLM transitions which were found (e.g. [26]) to be very sensitive to the coupling type (namely $KL_1M_{2,3}$, $KL_2M_{2,3}$ and $KL_3M_{2,3}$). The measured intensity ratios of these lines (obtained also from special measurements) agree within 2σ with those of the non-relativistic calculations in the intermediate coupling of Babenkov et al. [27] (including the $KL_{1-3}M_{1-3}$ transitions only) while the jj coupling values [25] are lower by 5σ and 12σ for the KL_1M_2/KL_1M_3 and $KL_2M_{2,3}/KL_3M_{2,3}$ intensity ratios, respectively (see Table 4b). For another intense KLM lines, the intensity ratios (e.g. KL_2M_1/KL_3M_1, KL_3M_2/KL_2M_3) predicted by both models are close to each other and to the experiment. Thus it is evident that the effect of intermediate coupling remains significant for the KLM spectrum still at Z=36. The disagreement between the theory [25] and our measurement found for other KLM transitions (or configurations) may be caused by the interaction of the final electron configurations. Up to our knowledge, this effect was not yet considered in the calculations of the KLM transition rates.

Table 4a

Relative energies and intensities of the KLX Auger transitions in krypton

Transition	Energies (eV)		Intensities (%)[a]		
	Experiment	Theory[b]	Experiment		Theory
	This work	Ref.16	This work	c	Ref.25
KL_1M_1	-322.1(5)	-319.9	7.0(3)		8.06
KL_1M_2	-246.4(9)	-244.8	6.9(5)	13.8(4)	4.59
KL_1M_3	-238.2(9)	-237.9	7.1(5)		7.50
KL_2M_1	-121.9(7)	-122.3	3.6(2)	4.3(2)	3.82
$KL_1M_{4,5}$	-114.9(10)	-115.0	1.1(2)		0.79
KL_3M_1	-71.0(6)	-71.1	4.3(2)		6.91
KL_2M_2	-58.2(9)	-58.1	1.5(2)	24.0(5)	1.43
KL_2M_3	-45.6(5)	-45.5	22.0(4)		14.91
KL_1N	-15.7(20)		0.7(3)		2.23
KL_3M_2	0.0	0.0	26.9(20)	33.2(6)	16.48
KL_3M_3	+7.6(14)	+4.6	6.4(15)		18.06
$KL_2M_{4,5}$	+76.1(5)	+76.1	2.8(2)		2.13
KL_3M_4	+125.5(7)	+125.5	2.5(2)	4.5(2)	2.42
KL_3M_5	+132.6(9)	+132.3	2.3(2)		2.45
KL_2N	+176.6(6)		2.1(1)		2.08
KL_3N	+228.7(7)		3.7(1)		6.01

[a] Normalized to ΣKLX.

[b] Energy differences between the $KL_3M_2(^3P_2)$ transition and the most intense one (according to ref.24) of a particular multiplet.

[c] Values obtained from the spectrum decomposition into ten components.

Table 4b

Intensity ratios of some KLM transitions in krypton

Ratio	Experiment	Theory	
	This work	Ref.27[a]	Ref.25
KL_1M_2 : KL_1M_3	0.91(6)	0.85	0.61
KL_2M_1 : KL_3M_1	0.83(8)	0.57	0.55
KL_3M_2 : KL_2M_3	1.22(8)	0.97	1.11
$KL_2M_{2,3}$: $KL_3M_{2,3}$	0.72(2)	0.76	0.47

[a] Values for Z=35.

In the case of the KLN spectrum, the greatest discrepancy is seen for the KL_3N transition; the predicted value exceeds the measured one by more than 14%. Our value of 5.8(2) for the $KL_{2,3}N$ component, however, agrees very well with that of 5.8(1.8) measured for Br(Z=35) [19].

KMX spectrum

In the evaluation of the KMX spectrum, the group of the $KM_{2,3}M_{2,3}$ transitions was also decomposed into three components (namely KM_2M_2, KM_2M_3 and KM_3M_3) as the fit by one line was unsatisfactory. Altogether, the relative intensities of thirteen KMX transitions or groups of transitions were determined as displayed in Table 5. The predictions presented are those of the relativistic calculations in *jj* coupling of Chen et al. [25], of the relativistic computations based on the intermediate coupling scheme with configuration interaction among all the possible final-double-MM-hole states of Chen et al. [28] and of our non-relativistic calculations in intermediate coupling with and without inclusion of the $(3s)^0(3p)^6$ and $(3s)^2(3p)^4$ configuration interaction (see ref.22 for more details).

As can be seen, the *jj* coupling treatment differs significantly from experiment; the discrepancies for the

Table 5

Relative energies and intensities of the KMX Auger transitions in krypton

Transition	Energies		Intensities (%)					
	Experiment	Theory[a]	Experiment		Theory[b]			
	This work	Ref.16	This work			This work[d]		
			c	b	Ref.25	e	f	Ref.28
$KM_1M_1(^1S_0)$	-149.1(9)	-151.1	5.1(3)	7.5(5)	11.8	8.9	7.3	9.7
$KM_1M_2(^1P_1)$	-82.1(9)	-84.2	13.2(7)	19.1(9)	11.8	21.7	21.7	22.8
$KM_1M_{2,3}(^3P)$	-64.6(12)	-65.1	5.5(5)	7.9(8)	18.3	5.1	5.1	7.1
$KM_2M_2(^1S_0)$	-9.8(13)	-9.1	3.4(9)	4.9(14)		4.2	5.2	5.4
KM_2M_3	0.0	0.0	37.7(31)[g]	54.7(45)	37.3	51.6	51.6	49.9
KM_3M_3	+13(2)	+10.4	4.1(10)	6.0(15)	20.9	8.6	9.3	5.1
$KM_1M_{4,5}$	+53.8(10)	+53.4	3.5(2)	5.0(2)				5.2
$KM_2M_{4,5}$	+118.0(9)	+113-127	6.7(5)	9.8(6)				8.1
$KM_3M_{4,5}+KM_1N$	+139.2(12)	+125-145	5.8(5)	8.4(7)	17.0			4.9[h]
$KM_{2,3}N_1$	+201.3(12)	+200-207	2.0(4)	2.9(5)	4.8			
$KM_{2,3}N_{2,3}+KM_{4,5}M_{4,5}$	+223.1(7)	+214-252	10.8(6)	15.6(7)	16.1[i]			0.2[h]
$KM_{4,5}N_1$	+315(3)	+326	1.0(6)	1.4(8)				
$KM_{4,5}N_{2,3}$	+346.9(16)	+342.6	1.5(4)	2.1(6)				

Table 5 - continued

[a] Energy differences between the $KM_2M_3(^1D_2)$ transition and the most intensive one of a particular multiplet.

[b] Normalized to $\Sigma KM_{1-3}M_{1-3}$.

[c] Normalized to ΣKMX.

[d] Non-relativistic calculations in the intermediate coupling (see text).

[e] Without configuration interaction.

[f] With configuration interaction.

[g] The value of 46.1(12) was obtained for the $KM_{2,3}M_{2,3}$ transition intensity from the fit by one line.

[h] The KM_1N_j transitions are not included.

[i] The $KM_{4,5}M_{4,5}$ transitions are not included.

individual lines (except the $KM_{2,3}N_{2,3} + KM_{4,5}M_{4,5}$ component) range from 40 to 130. It is evident, therefore, that the jj coupling scheme is unapplicable for the description of the KMX spectrum in this Z-region. The intermediate coupling calculations with configuration interaction give relatively good agreement with the measurement, especially the non-relativistic ones. The relativistic calculations overestimate the $KM_1M_1(^1S_0)$ and $KM_1M_2(^1P_1)$ transition rates and underestimate the KM_2M_3 one. For the corresponding configurations, the predicted intensities [28] differ similarly from the measured ones. Thus the intermediate coupling calculations of Chen et al. [28] deviate from experimental data in an analogous way as we observed for the calculations of Chen et al. [1] in the case of the KLL spectrum.

Groups

In Table 6, the measured KLX:KLL and KMX:KLL group intensity ratios are compared with those obtained from both the calculations [25,29] and the fits [30,31] to the experimental data. The predicted as well as fitted KLX:KLL values agree with the experimental one within the quoted error while for the KMX:KLL ratio, the agreement with our value within 10 is seen only for the calculations [25] (the calculations [29] include only KMM transitions). The fitted value [30] seems to be overestimated.

Table 6

Relative intensities of the K Auger groups of krypton

Ratio	Experiment	Theory			
	This work	Ref.25	Ref.29	Ref.30	Ref.31
KLX : KLL	0.336(12)	0.339	0.332	0.342	0.34(4)
KMX : KLL	0.029(2)	0.029	0.021[a]	0.038	0.025(9)

[a] Only the KMM group included.

REFERENCES

1 M.H. Chen, B. Crasemann and H. Mark, Phys. Rev. A, 21 (1980) 442.

2 M.I. Babenkov, B.V. Bobykin, V.S. Zhdanov and V.K. Petukhov, Izv. Akad. Nauk SSSR, 40 (1976) 2065 (in Russian).

3 M.I. Babenkov, B.V. Bobykin and V.S. Zhdanov, J. Electr. Spectrosc. Relat. Phenom., 31 (1983) 307.

4 Ch. Briancon, B. Legrand, R.J. Walen, Ts. Vylov, A. Minkova and A. Inoyatov, Nucl. Instrum. Methods, 221 (1984) 547.

5 D.K. Gibson and I.D. Reid, J. Phys. E: Sci. Instrum., 17 (1984) 443.

6 G.E. Borchert, Z. Naturforch. Teil A, 31 (1976) 387.

7 G.L. Borchert, W. Scheck and K.P. Wieder, Z. Naturforch. Teil A, 30 (1975) 274.

8 C.M. Lederer and V.S. Shirley, Tables of Isotopes (7th edn), Wiley, New York, 1978, Appendices-3.

9 M.A. Lee, Nucl. Data Sheets, 50 (1987) 604.

10 V.M. Gorozhankin, A. Kovalík, Li En Ir, M.A. Mahmoud, J. Novák and A.F. Novgorodov, Proc. 40th Conf. on Nuclear Spectroscopy and Nuclear Structure, Nauka, Leningrad, 1990, p. 97 (in Russian).

11 M. Ryšavý and M. Fišer, Comput. Phys. Commun., 29 (1983) 171.

12 A. Kovalík, A. Inoyatov, A.F. Novgorodov, V. Brabec, M. Ryšavý, Ts. Vylov, O. Dragoun and A. Minkova, J. Phys. B: At. Mol. Phys., 20 (1987) 3997.

13 V.N. Pokrovskij, A. Inoyatov, I.A. Prostakov, Ch. Briancon, Ts. Vylov, B. Legrand, A. Minkova and A.A. Pasko, Preprint P6-86-134, Dubna: Joint Institute for Nuclear Research, 1986 (in Russian).

14 V.I. Nefedov, X-ray Photoelectron Spectroscopy of Chemical Compounds, Handbook , Khimija, Moscow, 1984, (in Russian).

G.S. Fadley, S.B.M. Hadstrom, M.P. Klein and D.A. Shirley, J. Chem. Phys., 48 (1968) 3779.

15 K.D.Sevier, Low Energy Electron Spectroscopy, Wiley, New York, 1972, p. 356.

16 F.P. Larkins, At. Data Nucl. Data Tables, 20 (1977) 311.

17 V.M. Gorozhankin, A. Kovalík, M.A. Mahmoud, A. Minkova, to be published.

18 A. Kovalík, M. Rýsavý, V. Brabec, O. Dragoun, A. Inoyatov, A.F. Novgorodov, Ts. Vylov and A. Minkova, J. Electr. Spectrsc. Relat. Phenom., 43 (1987) 225.

19 P. Erman, I. Bergstrom, Y.Y. Chu and T. Emery, Nucl. Phys., 62 (1965) 401.

20 M.O. Krause and J.H. Oliver, J. Phys. Chem. Ref. Data, 8 (1979) 329.

21 M.I. Babenkov, B.V. Bobykin and V.K. Petukhov, Izv. Akad. Nauk SSSR, 36 (1972) 2139.

22 A. Kovalík, V. Brabec, J. Novák, O. Dragoun, V.M. Gorozhankin, A.F. Novgorodov and Ts. Vylov, J. Electr. Spectrosc. Relat. Phenom., 50 (1990) 89.

23 M.H. Chen and B. Crasemann, Phys. Rev. A, 8 (1973) 7.

24 W.N. Asaad and E.H.S Burhop, Proc. Phys. Soc., 71 (1958) 369.

25 M.H. Chen, B. Crasemann and H. Mark, At. Data Nucl. Data Tables, 24 (1979) 13.

26 M.I. Babenkov, V.S. Zhdanov and S.A. Starodubov, J. Phys. B: At. Mol. Phys., 19 (1986) L563.

27 M.I. Babenkov, V.S. Zhdanov and S.A. Starodubov, Proc. 36th Conf. on Nuclear Spectroscopy and Nuclear Structure, Nauka, Leningrad, 1986, p. 267 (in Russian).

28 M.H. Chen, B. Crasemann and H. Mark, Phys. Rev. A, 27 (1983) 1213.

29 E.J. McGuire, Phys. Rev. A, 2 (1970) 273.

30 P.V. Rao, M.H. Chen and B. Crasemann, Phys. Rev. A, 5 (1972) 997.

31 M.I. Babenkov, V.S. Zhdanov, V.K. Petukhov and S.A. Starodubov, Preprint 6-85, Alma-Ata: Nuclear Physics Institute, 1985 (in Russian).

Received by Publishing Department
on October 22, 1990.